BL-8B/2021G534

Magnetostriction related to skyrmion-lattice formation in chiral magnet FeGe

Masaki MITO[1,*] and Takayuki TAJIRI[2]
[1] Kyushu Institute of Technology, Kitakyushu 804-8550, Japan
[2] Fukuoka University, Fukuoka 814-0180, Japan

The cubic type chiral magnet FeGe exhibits the formation of skyrmion-lattice (SkL) phases near the magnetic ordering temperature. The SkL is composed of vortex-type spin objects, and it is a kind of magnetic superlattice. Through the X-ray diffraction analyses for the single crystal, we observed the spin–orbit coupling induced magnetostriction related to the SkL formation. The phase diagram near the magnetic ordering temperature was reconstructed from the prospect of the magnetostriction.

1 Introduction

Crystallographic chirality is transferred into the spin chirality via a Dzyaloshinskii-Moriya (D–M) interaction [1, 2], so that the helimagnetic (HM) spin alignment is stabilized below a magnetic ordering temperature (T_c). Furthermore, a finite dc magnetic field (H_{dc}) stabilizes a chiral spin texture composed of topological spin objects below T_c [3]. In B20 type chiral magnets with non-centrosymmetric crystal structure, such as MnSi [4, 5], $Fe_{1-x}Co_xSi$ [6], and FeGe [7], the D–M interaction, thermal fluctuation, and Zeeman energy stabilize the Bloch type skyrmion lattice (SkL) state in the immediate vicinity of T_c. The SkL phase is a hexagonal skyrmion crystal, and the low-temperature side of the SkL phase is surrounded with the conical magnetic (CM) phase.

We believed that in the process of SkL phase formation, the crystal lattice should be affected by any severe strain, followed by a change in the lattice parameters as a function of H_{dc} and temperature (T). The origin of the D–M interaction is the spin-orbit coupling. Indeed, magnetostriction driven by spin–orbit coupling has already been observed in chiral magnets such as $CrNb_3S_6$ [8-10], MnSi [11], and Cu_2OSeO_3 [12]. These magnetostriction experiments prove that structural analysis can be employed as an experimental approach for elucidating the complex magnetic phase diagram originating from the spin-orbit coupling. This study demonstrated the magnetostriction phenomena in FeGe to obtain valuable insights about the influence of SkL formation on the lattice system so that we reconstructed the detailed $H_{dc}-T$ phase diagram near T_c.

FeGe has a cubic structure with the space group $P2_13$, and it has a magnetic order near room temperature and exhibits the SkL phase for $0.1 < H_{dc} < 0.6$ kOe. A $H_{dc}-T$ phase diagram for FeGe near T_c had been studied experimentally using ac susceptibility and heat capacity measurements [13, 14]. According to the literatures [13, 14], the SkL phase is divided into four regions of A_n (n = 0 - 3). It is meaningful to distinguish many phases from each other via the prospect of how the crystal lattice experiences changes in its magnetic properties.

2 Experiment

A single crystal of FeGe was grown via a chemical vapor transport technique using iodine I_2 as the transporting agent [15, 16]. The largest flat plane was perpendicular to the [001] direction. In this experiment, the $H_{dc}-T$ phase for the present single crystal of FeGe was first verified through the H_{dc} dependence of ac magnetization, which could be observed using a commercial superconducting quantum interference device magnetometer with an ac option [17].

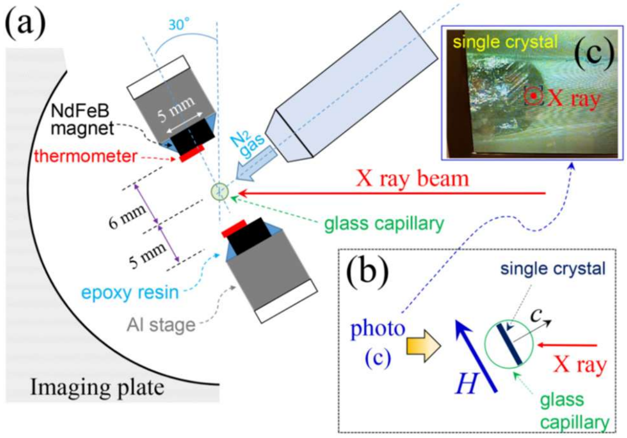

Fig. 1: (a) Experimental setup for the XRD experiments with the parameters of T = 265–305 K and H_{dc} = 0–1.04 kOe [17]. (b) Setup of a single crystal ($c \perp H_{dc}$) in glass capillary and (c) a sample photo in the setup of (b).

The XRD experiments were conducted in the temperature region of 265–305 K using a synchrotron radiation XRD system with a cylindrical imaging plate at the Photon Factory, BL-8B, at the Institute of Materials Structure Science, High Energy Accelerator Research Organization [18]. The incident x-ray energy was 16 keV. The temperature of the sample was measured using a K-type chromel–alumel thermocouple. Two NdFeB magnets (NeoMag Co., Ltd.: Product No. N48H with a remanence of 13.8 kG and a size of 10 × 6 × 3 mm^3 and Product No. N52 with a remanence of 14.5 kG and a size of 10 × 7 × 8 mm^3) were placed in the aforementioned diffractometer as shown in Fig. 1(a) [17]. Furthermore, the phase diagram of FeGe below T_c is not independent of the direction of H_{dc}, particularly in the *ab*-plane [13, 14, 19]. In this study, the X ray passed through the thin edge of the crystal. Consequently, H_{dc} was applied perpendicularly to [001] as shown in Fig. 1 (b). According to the literature [20], the phase diagram concerning the SkL phase for H_{dc} // [001] is consistent with that for H_{dc} // [110]. The H_{dc} values were changed by controlling the distance between the sample and NdFeB magnets. Subsequently, H_{dc} was always reduced to zero before constructing a new configuration of NdFeB magnets. More than 50 diffraction spots for single crystals were observed in the vibration mode every 1° for -5° ~ +5°. Based on the distances between the spots, changes in the lattice constant were evaluated using the least-squares method.

3 Results and Discussion

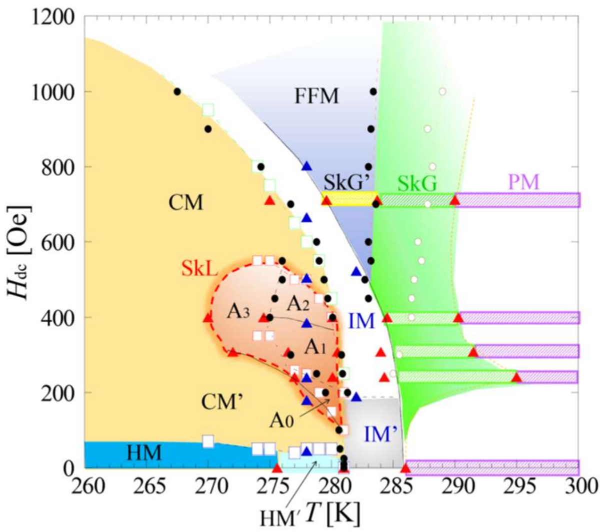

Fig. 2: Phase diagram of FeGe near T_c recognized by the XRD experiments (red ▲: T-scan, blue ▲: H_{dc}-scan), along with the results of ac magnetization [in-phase $m'(H_{dc})$: □, $m'(T)$: ●, out-of-phase $m''(T)$: ○] [17]. Through the present XRD experiments as a function of T and H_{dc}, certain precursor phases, such as HM', IM', IM, and SkG, are successfully classified. In $m'(T)$, A_3 is observed, and precursor phase IM is also detected. The border between SkG' and SkG is also detected by $m'(T)$ and $m''(T)$, whereas that between SkG and PM cannot be verified by $m'(T)$ and $m''(T)$. The boundary between IM and SkG and that between IM' and PM can be determined from the crossover in the T dependence of m': Both IM and IM' exhibit the linearity in the T dependence of $m'(T)$, while both SkG and PM does the Curie–Weiss like $m'(T)$.

We constructed a new phase diagram on FeGe as Fig. 2 according to the following procedures: (1) First, the primary phase diagram is prepared via m'-H_{dc} measurements, and the outlines of CM, SkL, and HM are drawn. In this case, we cannot draw an outline of the IM phase. (2) Second, through an XRD experiment as a function of T at some fixed H_{dc}'s, the HM and SkL phases are divided into some phases. For instance, the HM phase is divided into two regions, one of which is HM' just below T_c. The SkL-A_3 phase occupies the low-T region of the SkL phases and it exists in the low-T side of A_1 and A_2. The region of the IM phase is confirmed through lattice elongation. In addition, in the T region between IM and ordinary PM phases, the SkG phase is observed, and it accompanies the minimum value in a due to the attraction between skyrmions. Furthermore, at H_{dc}. 700 Oe, the SkG' phase, which is different from both IM and SkG, is accompanied by lattice contraction in the cooling process. Consequently, this SkG' phase is identified as the same phase as the FFM phase. (3) Third, through the XRD experiment as a function of H_{dc} at two T values, the SkL phases are separated into A_0, A_1, and A_2, and the IM phases are also divided into two phases, IM and IM'. (4) Finally, via the m'–T measurements at many H_{dc}'s, the boundaries between CM (CM') and A_0, between A_3 and $A_{1,2}$, between IM and CM, between IM and $A_{0,1,2}$, between HM' and IM', between CM (CM') and IM', and between SkG' (FFM) and SkG are reconfirmed. Using the aforementioned approach, HM', IM', and SkG have been newly detected. Even at H_{dc} = 0, the HM phase is not uniform, and the region just below T_c is distinguished as the HM' phase from the genuine HM phase in the low-T side. Below the critical H_{dc} value required for stabilization of the SkL phase, the so-called IM phase is distinguished as the IM' phase from the IM phase above the critical H_{dc}. The IM' phase appears in the high-T side of HM', which is the precursor state of the HM phase. The IM' phase is surely the short-range ordering of the HM spin texture like one-dimensional HM nematic phase. SkG located on the high-T side of the IM phase exhibits the minimum in a, and this phase cannot be verified by m' and m''. IM located on the high-T side of SkL phases exhibits a maximum a, which is phenomenologically similar to the phenomenon in the solidification of water molecules. Indeed, the increase in a for IM is compensated by the decrease in a for SkG. The appearance of SkG, IM, and SkL requires H_{dc} above a certain threshold field H_c. At much larger H_{dc} than H_c, there is a tri-critical point surrounded with IM, FFM (SkG'), and SkG. Both SkL-A_1 and A_2 exhibit a constant T dependence on a, whereas a of A_3 varies with changes in H_{dc}. In particular, the SkL formation indicates the various magnetostriction effects. It is important to recognize that the lattice experiences significant stress via the SkL formation in various ways. Thus, the phase diagram of FeGe as a function of T and H_{dc} is complex. SkL is composed of various phases, such as A_0–A_3, which exhibit a magnetostriction unique to each phase. The IM phase can also be separately characterized into two regions with a threshold of approximately 200 Oe. The SkG is also stabilized for H_{dc} above approximately 200 Oe. Consequently, we can recognize the importance of the critical H_{dc} field for the formation of a magnetic superlattice composed of skyrmions. This new knowledge was obtained from the magnetostriction phenomena induced by a strong magnetostructural correlation. Microscopic data at the unit-cell level reveal that even the IM region is not uniform. Moreover, on the higher-T side of the SkL phase, a structurally fluctuating T region exists, similarly to a previous study on MnSi [21]. To stabilize the SkL phases, many phases that accompany lattice elongation and contraction exist.

Acknowledgement

We thank many collaborators, Prof. Y. Kousaka, Prof. J. Akimitsu, and Prof. K. Inoue, in the present study.

References

[1] I. E. Dzyaloshinskii, *J. Phys. Chem. Solids* 4, 241 (1958).
[2] T. Moriya, *Phys. Rev.* **12**0, 91 (1960).
[3] A. N. Bogdanov and C. Panagopoulos, *Phys. Today* **73**, 44 (2020).

[4] S. Mühlbauer, B. Binz, F. Jonietz, C. Pfleiderer, A. Rosch, A. Neubauer, R. Georgii, and P. Böni, *Science* **323**, 915 (2009).
[5] T. Adams, S. Münhlbauer, C. Pfleiderer, F. Jonietz, A. Bauer, A. Neubauer, R. Georgii, P. Böni, U. Keiderling, K. Everschor, M. Garst, and A. Rosch, *Phys. Rev. Lett*. **107**, 217206 (2011).
[6] X. Z. Yu, Y. Onose, N. Kanazawa, J. H. Park, J. H. Han, Y. Matsui, N. Nagaosa, and Y. Tokura, *Nature* **465**, 901 (2010).
[7] X. Z. Yu, N. Kanazawa, Y. Onose, K. Kimoto, W. Z. Zhang, S. Ishiwata, Y. Matsui, and Y. Tokura, *Nat. Mater.* **10,** 106 (2011).
[8] T. Tajiri, M. Mito, Y. Kousaka, J. Akimitsu, J. Kishine, and K. Inoue, *Phys. Rev. B* **102**, 014446 (2020).
[9] M. Mito, T. Tajiri, Y. Kousaka, Y. Togawa, J. Akimitsu, J. Kishine, and K. Inoue, *Phys. Rev. B* **105**, 104412 (2022).
[10] M. Mito, T. Tajiri, Y. Kousaka, J. Akimitsu, J. ichiro Kishine, and K. Inoue, *Phys. Rev. B* **107**, 054427 (2023).
[11] S. Wang, Y. Hu, J. Tang, W. Wei, J. Cong, Y. Sun, H. Du, and M. Tian, *New J. Phys.* **21**, 123052 (2019).
[12] P. Dutta, M. Das, A. Banerjee, S. Chatterjee, and S. Majumdar, *J. Alloys Comp*. **886**, 161198 (2021).
[13] H. Wilhelm, M. Baenitz, M. Schmidt, U. K. Rößler, A. A. Leonov, and A. N. Bogdanov, *Phys. Rev. Lett*. **107**, 127203 (2011).
[14] H. Wilhelm, M. Baenitz, M. Schmidt, C. Naylor, R. Lortz, U. K. Rößler, A. A. Leonov, and A. N. Bogdanov, *J. Phys.: Condens. Matter* **24**, 294204 (2012).
[15] M. Richardson, *Acta Chem. Scand*. **21**, 2305 (1967).
[16] A. Leonov, Y. Togawa, T. Monchesky, A. Bogdanov, J. Kishine, Y. Kousaka, M. Miyagawa, T. Koyama, J. Akimitsu, T. Koyama *et al*., *Phys. Rev. Lett*. **11**7, 087202 (2016).
[17] M. Mito, T. Tajiri, Y. Kousaka, M. Miyagawa, T. Koyama, J. Akimitsu, and K. Inoue, *J. Appl. Phys*. **136**, 123902 (2024).
[18] A. Fujiwara, K. Ishii, T. Watanuki, H. Suematsu, H. Nakao, K. Ohwada, Y. Fujii, Y. Murakami, T. Mori, H. Kawada *et al*., *J. Appl. Cryst.* **33**, 1241 (2000).
[19] E. Turgut, M. J. Stolt, S. Jin, and G. D. Fuchs, *J. Appl. Phys*. **122**, 183902 (2017).
[20] E. Moskvin, S. Grigoriev, V. Dyadkin, H. Eckerlebe, M. Baenitz, M. Schmidt, and H. Wilhelm, *Phys. Rev. Lett*. **110**, 077207 (2013).
[21] K. Tsuruta, M. Mito, H. Deguchi, J. Kishine, Y. Kousaka, J. Akimitsu, and K. Inoue, *Phys. Rev. B* **97**, 094411 (2018).

* mitoh@mns.kyutech.ac.jp